Experimental Studies on Regime Mapping of a Rising Bubble

Dilin Sharaf M

A Thesis Submitted to
Indian Institute of Technology Hyderabad
In Partial Fulfillment of the Requirements for
The Degree of Master of Technology

भारतीय प्रौद्योगिकी संस्थान हैदराबाद
Indian Institute of Technology Hyderabad

Department of Mechanical Engineering

June 2016

Declaration

I declare that this written submission represents my ideas in my own words, and where ideas or words of others have been included, I have adequately cited and referenced the original sources. I also declare that I have adhered to all principles of academic honesty and integrity and have not misrepresented or fabricated or falsified any idea/data/fact/source in my submission. I understand that any violation of the above will be a cause for disciplinary action by the Institute and can also evoke penal action from the sources that have thus not been properly cited, or from whom proper permission has not been taken when needed.
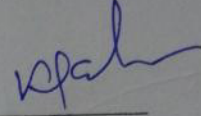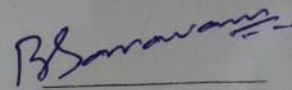
(Signature)

Dilin Sharaf M

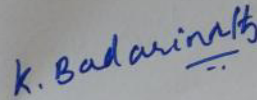(Dilin Sharaf M)

MEIAMTECH11004

(Roll No.)

Approval Sheet

This Thesis entitled Experimental Studies on Regime Mapping of a Rising Bubble by Dilin Sharaf M is approved for the degree of Master of Technology from IIT Hyderabad
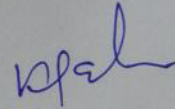
(Dr K C Sahu) Examiner
Dept. of Chem Eng
IITH

(Dr Saravanan B) Examiner
Dept. Mech and Aero Eng
IITH

(Dr Karri Badarinath) Adviser
Dept. of Mech and Aero Eng
IITH

(Dr K C Sahu) Chairman
Dept. of Chem Eng
IITH

Acknowledgements

Abstract

An experimental study on shape variation of an initially spherical rising bubble in different liquids is presented, which validates the results from a paper by Tripathi et al.[2]. They had presented numerical simulation of an initially spherical gas bubble rising in a viscous fluid by Volume of Fluid method with a finite volume open source code, Gerris. They put forward the existence of a phase plot in Eotvos - Galilei plane having five different regimes of bubble behavior with well defined boundaries. The regimes are characterized by differences in the shape of rising bubble (for example ellipsoidal, axisymmetric cap with a skirt and a doughnut like shape) as well as the path traversed by it (for example straight, zigzag and spiral path). The regime a bubble falls in depends on both its Eotvos and Galilei numbers. In the present study an experimental setup was developed to create an initial bubble of different sizes in a liquid and observe its rise behavior using a high-speed camera. This setup enabled us to get a 2D image of shape and path oscillation through high-speed video recordings. Aqueous glycerol solutions of different volume concentrations were used to obtain the range of Eotvos and Galilei numbers as presented by Tripathi et al [2]. The results indicate that at low Ga and Eo the bubbles show similar path and shape behavior and show the demarcation of regime boundaries as the numerical simulation. But at high Ga and Eo, there is a mismatch in terms of the regime demarcation boundary indicating that initial condition of the bubble is a critical parameter.

Contents

List of Figures

viii

Nomenclature

Bo	Bond Number
cP	centi Poise
Eo	Eotvos Number
fps	frames per second
g	Acceleration due to Gravity ($9.81 m/s^2$)
Ga	Galilei Number
K	Kelvin
MΩ	Mega Ohm
Mo	Morton Number
R	Radius
Re	Reynolds Number
t	time
t^*	Non-dimensional Time given as $t^* = t \times \sqrt{9.81/R}$
v	Velocity
We	Weber Number
μ	Dynamic Viscosity
μ_i	Dynamic Viscosity of Dispersed phase
μ_o	Dynamic Viscosity of Continuous phase
μ_r	Ratio of Dynamic Viscosity given as μ_i/μ_o
ρ	Density
ρ_i	Density of Dispersed phase
ρ_o	Density of Continuous phase
ρ_r	Density ratio given as ρ_i/ρ_o
σ	Surface Tension

Chapter 1

Introduction

Bubbles and drops are universal in nature and play critical roles in many important natural physical processes and several industrial processes. Some examples include their role in rain, thermal budget of the atmosphere, chemical and biological dispersion, volcanoes and exploding lakes, and disease transmission [3]. Meteorologists and geophysicists have studied the behavior of raindrops and hailstones, chemical and metallurgical engineers have focused on bubbles and drops for processes like distillation, absorption, and floatation etc. while mechanical engineers studied the droplet behavior for clearly explaining the combustion processes [4].

A bubble or drop is commonly influenced by gravitational, surface tension, and viscous forces. In addition occasionally, there may be electric, magnetic and other forces. The effect of these forces results in different bubble and drop behaviors, depending on bubble or drop size, density and viscosity of the fluids involved. A bubble is defined as a blob of low density fluid inside a relatively denser medium. In nature the bubbles may form in water through exsolution of dissolved gases. For example, while raining when the raindrops hit the water surface the air entrapped causes bubble formation on the water surface. They can also form through cavitation because of vigorous flow. The lifetime of a bubble in a particular fluid is limited by its dissolution with the surrounding fluid. A drop can be considered as a blob of high density fluid inside a relatively lower density medium. Droplet formation in the atmosphere arises due to the condensation of water vapor in the form of rain and dew. The lifetime of a water drop falling down in atmosphere is limited by evaporation, however there is a chance for coalescence with other drops and further condensation. It is observed that droplets impacting on a free surface cause the formation of underwater bubbles, and likewise bubbles bursting on the free surface of a fluid cause the formation of tiny droplets.

There are mainly three types of bubbles found in nature, they are (i) encapsulated bubble in which some gas is enclosed by a thin fluid film, (ii) a gas bubble in which a blob of low density gas is entrapped in a high density medium, and (iii) cavitation bubbles which are formed by rapid changes in pressure in a flow field and that causes the formation of cavities with a relatively lower pressure. Soap bubble is a good example for encapsulated bubble with a thin layer of soap separating the inside air from outside air. Encapsulated bubble have wide applications in medical field such as in ultrasound imaging where small encapsulated bubbles called contrast agents are used to enhance the contrast of the imaging. The contrast agents are made from either a lipid or a protein [5] . Cavitation bubble is a non-equilibrium bubble [6], since there exist some pressure difference between interior

and exterior of the bubble. Because of this pressure difference these bubble shows the oscillatory behavior. Cavitation is mainly divided into two classes of behavior. One is inertial cavitation, where a void formed in the liquid rapidly collapses and produces a shock wave, like we can see in pumps, propellers and impellers. The other kind is non-inertial cavitation in which a bubble in a fluid show radial oscillation in size or shape without collapsing. These kind of cavitation are often employed in ultrasonic cleaning.

As seen above the bubbles can occur in many situations including natural processes (like aerosol transfer from sea and electrification of atmosphere by sea bubbles [7]), industrial processes (like petroleum refining and mineral industries [8]) and also for some biomedical and environmental applications including drug transport, environmental sensing [3]. For utilizing bubbles in these applications properly a detailed study of dynamics of bubble such as nucleation and inception of bubble, radial oscillation, oscillation frequency, rise velocity, shape variation and the path it follows are needed.

In the context of a rising bubble lots of research has been done to analyze the shape, trajectory and terminal velocities of a rising bubble. All those studies mainly focused on the rise velocity, path instability, bubble shapes and to derive models for estimating different bubble parameters. Most of them were restricted to a short range of Galileo and Eotvos numbers. In this study we focus on the dynamics of a single gas bubble rising in a viscous fluid under gravity for a wide range of Galilei and Eotvos numbers.

1.1 Literature Review on Rising Bubble in a Liquid

The dynamics of rising gas bubble mainly depends upon the surface tension, viscous force, buoyancy force and density. The earliest documented mention of study of rising bubble motion has been found in a manuscript, Codex Leicester, by Leonardo Da Vinci, discovered by Prosperetti [9]. Da Vinci described the spiral motion of bubbles (Leonardo's Paradox) when released axisymmetrically from the bottom of a container filled with water which is basically the path instability of bubble. A popular shape regime chart for low density and viscosity ratio fluid blobs has been presented by Clift et al. [4]. Since in this work we are trying to classify bubbles into different regimes based on path and shape instability, we now review some relevant papers in greater detail.

Jinsong et al. [10] have done a numerical study of a 3D bubble rising in a viscous liquid. They solved the flow field on a fixed grid and tracked the interface position in a Lagrangian manner which is referred to as a front tracking method. And they validated this against experiments over a range of Bond (Eotvos) and Reynolds numbers. The solution method followed was a finite volume based SIMPLE scheme. They found that the new SIMPLE algorithm is robust with larger range of Reynolds number, Bond number, density ratio and viscosity ratio.

Smolianski et al. [11] did a computational and experimental study on the dynamics of a rising gas bubble in viscous liquids. They succeeded in simulating the shape of the deforming interface of the gas bubble and surface tension effects. They presented the unsymmetrical vortex path of the high Reynolds number wobbling bubble regime clearly. The simulated position and rise velocity and different shape regimes of the bubble showed a clear validation of the experimental results.

One of the first studies in the field of experimental gas bubble dynamics was done by Bhaga et al. [1], where they studied the bubble shape terminal velocity and the wake associated with it. In their experiments the bubble is allowed to rise in transparent plexiglass column filled with aqueous sugar solutions of different concentration. For creating bubbles a known volume of air from a calibrated syringe is collected in a hemispherical dumping cup and then allowed to rise as a single bubble through the test section. They captured the rising bubble by means of a cine camera which is moving upward at the same speed as that of the bubble with the help of some electronic circuits. By using hydrogen bubbles the velocity field around the bubble has been visualized. These tracer bubbles were illuminated by means of a diffused backlighting method. They classified the shapes of the bubbles got through their experiments as spherical, oblate ellipsoidal, oblate ellipsoidal cap, spherical cap with open or closed wake and skirted bubbles with smooth or wavy skirt. The images of those bubbles are shown in Figure 1.1 From their studies on drag and wake associated with a rising bubble, they found that for liquids with Morton number greater than 4×10^{-3} the bubble shape, wake patterns and the drag coefficient depends only on Reynolds number.

Liu et al. [12] studied about single bubble dynamics in water and aqueous glycerol solution. They found that apart from bubble diameter, the nozzle diameter also influences the bubble shape trajectory and terminal velocity. The smaller bubble attains a spherical shape and rises vertically upward without any oscillation. But the larger ones deforms to ellipsoidal, oblate ellipsoidal or cap shape with a zigzag or helical motion. The bubbles in water are mainly influenced by inertial force and surface tension, while in glycerol viscous force also affects its behavior.

Haberman et al. [13] did an experimental study on the shape and drag of an air bubble. They conducted experiments on a single air bubble rising in various liquids to study its shape. The shapes of the bubbles they observed were spherical, ellipsoidal, and spherical cap. In the case of

(a)
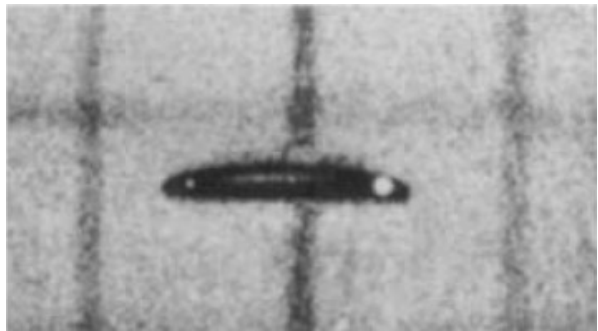
(b)
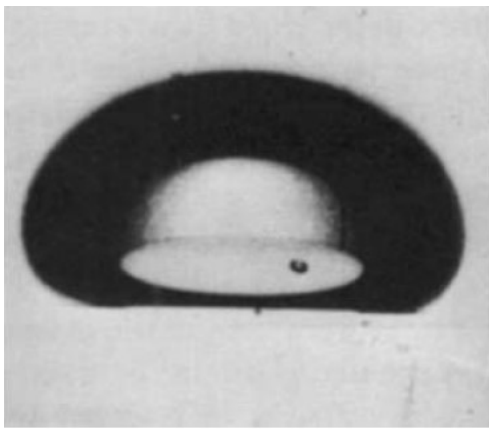
(c)
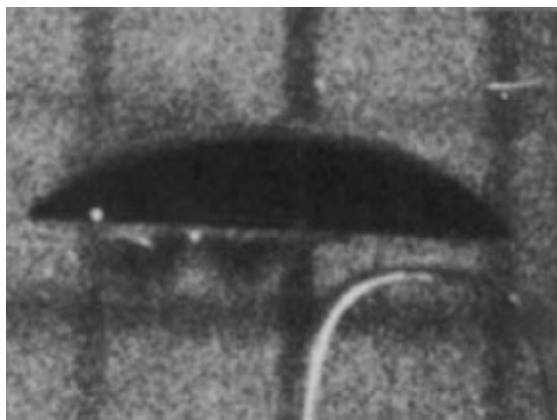
(d)

(e)

Figure 1.1: (a) Spherical bubble, (b) Disk shaped bubble, (c) Oblate ellipsoidal cap bubble, (d) Spherical cap bubble, (e) Skirted bubble, Figure taken from Bhaga et al [1] with permission. © The Journal of Fluid Mechanics.

drag coefficient, for a spherical bubble it coincides with that of the corresponding rigid sphere and it reduces as the bubble size increases. The drag coefficient of spherical cap bubbles are independent of the bubble size with a constant value of 2.6. Their experiments consisted of measuring the terminal velocities of a single bubble of various sizes in eight different liquids, and the determination of wall effects on the terminal velocity. To analyze the effect of walls they did the experiments in 3 test tanks of different dimensions. They concluded their work as, for spherical bubbles, viscosity plays a major role in determining the terminal velocity but for ellipsoidal bubbles, surface tension has greater importance and the spherical cap bubbles are independent of the fluid properties.

Hartunian et al. [14] investigated the instability of gas bubbles moving uniformly in various liquids experimentally and theoretically. They conducted the experiments to postulate Weber number should be a significant parameter involved in the stability of gas bubbles rising in liquids. The experimental results show that, the instability of the bubble arises due to interaction of surface tension and hydrodynamic pressure, and the lateral motion is caused by an interaction between capillary shape oscillations and the translation of the bubble.

The surfactant effect on path instability of a rising bubble has been studied by Tagawa et al. [15]. They captured the nitrogen bubbles rising in a test tank filled with Millipore water with the help of two digital cameras kept perpendicular to each other for analyzing the bubble in 3 dimensions. The size of the bubbles they studied lie within the range of 1 to 4 mm diameter. They found that the addition of surfactant leads to Marangoni effect which in turn varies the surface slip condition from free-slip to no-slip condition. They also observed the three dimensional motion of the bubble behaved in different manner with change in surfactant concentration. They have observed a new trajectory namely the transition between helical to a zigzag manner. Finally they succeeded in classifying the parameter ranges to get straight, helical or zigzag motion and plotted in a $Re - C_D$ space.

Lunde and Perkins [16] have conducted a detailed experimental study on shape and motion parameters of a bubble rising in tap water with the help of high speed cinematography and digital image processing. The effect of nozzle diameter on bubble size were carried out by injecting bubbles through nozzles of different diameter. The three dimensional images were obtained by using a high-speed camera and a mirror setup. They found that as the size of the bubble increases the oblate spheroid shape bubble rises in a wobbly and spiraling manner.

In this particular study we are going to experimentally validate the numerical results from the paper Dynamics of an initially spherical gas bubble rising in quiescent liquid by Tripathi et al. [2]. Specifically it is a study on shape variation of an initially spherical rising bubble in liquids of different physical properties. As size of the bubble changes, its shape and motion will behave differently in different liquids. They plotted these numerical results on a Galileo Eotvos plane with five different regions. Our main attempt is to experimentally replicate this phase plot.

1.2 Key Contribution

Before going into details of our work, the key contribution of this thesis are presented below.

- Most of the previous works on rising bubble were focused only few Eotvos and Galilei numbers. In this work we extended the range of Eotvos and Galilei numbers from 0.1 to 200 and 7 to 500 respectevly.

- We have fabricated an experimental setup to create bubbles of variable sizes in fluids of different viscosity with the help of a dumping cup mechanism and aqueous glycerol solutions.

- We used a highspeed camera, to provide good quality pictures and videos of rising bubble.

- Numerical results of Tripathi et al.[2] have been validated through our experimental study with some mismatch at higher Galilei and Eotvos numbers.

1.3 Structure of the Thesis

After giving a brief introduction to gas bubble dynamics in Chapter 1, we present a detailed background of Tripathi et al.'s [2] work, which the current study seeks to experimentally validate in Chapter 2. This mainly comprises the description of five different regimes of Eotvos Galilei phase plot put forward by Tripathi et.al. [2]. The non-dimensional parameters used for their simulation is also presented in this context. Chapter 3 discusses the experimental setup fabricated and methodology followed. The properties of aqueous glycerol solutions (which were used to obtain the ranges of Eotvos and Galilei numbers) of different samples are also presented here. And later, the detailed procedure of experiments is mentioned. In Chapter 4, the characteristics of different bubble behavior along with the images captured by high-speed camera are described. Chapter 5 provides conclusion of thesis and scope of future work. We also discuss the reason for differences in our experimental and Tripathi et al.'s [2] simulation results.

Chapter 2

Background: Numerical Simulation on a Rising Gas Bubble

The present thesis reports experimental work on the shape and path of a rising gas bubble. A key motivation in this study was to check whether we can experimentally observe the gas bubble behavior as reported in a simulation study by Tripathi et al. [2]. To better appreciate the present experimental results, we present some details about Tripathi et al.'s [2] simulation results as a background to our experimental study.

2.1 Non-dimensional numbers affecting rising gas bubble dynamics

The important physical properties that affect a bubble rising in a viscous fluids are density (ρ), viscosity (μ), and surface tension (σ). Apart from that the acceleration due to gravity (g) and the radius of the bubble (R) also play an important role in deciding the nature of rising bubble and its dynamics. As the size of the bubble changes, its dynamics changes abruptly from one class of shape and motion to another kind of shape and motion and further increase in size results in the breakup of the bubbles. In the numerical simulation of rising gas bubble Tripathi et al [2]. used four non-dimensional parameters. They are Galilei number (Ga), Eotvos number (Eo), density ratio (ρ_r) and viscosity ratio (μ_r).

Galilei number is denoted as Ga and is defined by the ratio of gravitational force to viscous force. The Galilei number become significant for cases like viscous flow and thermal expansion calculations, for example, to describe the fluid film flow over the walls and to describe the dynamics of a rising bubble.

$$\text{Galilei number}, \text{Ga} = \frac{\text{gravitational force}}{\text{viscous force}} = \frac{\rho_0 R \sqrt{gR}}{\mu_0} \tag{2.1}$$

Eotvos number is denoted as Eo and is defined by the ratio of gravitational force to surface tension force. It is also called as Bond number Bo. Generally the Eotvos number is significant in the case of momentum transfer problems, and in particular it is used in the atomization and motion

of bubbles and drops calculations.

$$\text{Eotvos number}, \text{Eo} = \frac{\text{gravitational force}}{\text{surface tension force}} = \frac{\rho_0 g R^2}{\sigma} \tag{2.2}$$

Generally for all multiphase flows where there is an interface between two different fluids, in order to analyze the fluid flow the important non-dimensional parameters used are Reynolds number Re and Weber number We.

$$\text{Reynolds number}, \text{Re} = \frac{\text{Inertia force}}{\text{Viscous force}} = \frac{\rho_0 R v}{\mu} \tag{2.3}$$

$$\text{Weber number}, \text{We} = \frac{\text{Inertia force}}{\text{surface tension force}} = \frac{\rho_0 R v^2}{\sigma} \tag{2.4}$$

But in the case of a gas bubble rising in a viscous fluid, its terminal velocity is not constant throughout its motion and this terminal velocity term is an unknown value. So in these cases this velocity term is replaced by gravity velocity term $\sqrt{gR}$ which is a constant value throughout the motion of the bubble and is a known value. If the terminal velocity term is replaced by gravity velocity term, the Reynolds number becomes Galilei number and the Weber number becomes Eotvos number.

The other two non-dimensional parameters important for a rising bubble problem are density ratio and viscosity ratio.

$$\text{Density Ratio}, \rho_r = \frac{\text{density of dispersed phase}}{\text{density of continuous phase}} = \frac{\rho_i}{\rho_0} \tag{2.5}$$

$$\text{Viscosity Ratio}, \mu_r = \frac{\text{Dynamic viscosity of dispersed phase}}{\text{Dynamic viscosity of continuous phase}} = \frac{\mu_i}{\mu_0} \tag{2.6}$$

In their numerical simulation Tripathi et al. [2] chose the density ratio as $\rho_r = 0.001$ and viscosity ratio as $\mu_r = 0.01$. This roughly corresponds to the air-water system where air is the dispersed phase and water the continuous phase.

The Galilei and Eotvos number depends upon the radius of the bubble. As the size of the bubble changes these two numbers also change. So there is one more non-dimensional number known as Morton number which is independent of the size of the bubble and is defined by

$$\text{Morton number}, \text{Mo} = \frac{Eo^3}{Ga^4} = \frac{g\mu_0^4}{\rho_0 \sigma^3} \tag{2.7}$$

Morton number depends only on the physical properties of the fluid. So Morton number will be a constant for a particular liquid-gas system.

2.2 Rising bubble phase plot

Tripathi et al. [2] have done numerical simulation of an initially spherical bubble rising in a viscous fluid. They changed the physical properties of the fluid in each simulation. The behavior of the bubble is found to be changed as the fluid and the size of the bubble is changed. They illustrated their results graphically in a logarithmic phase plot with axes as Eotvos number and Galilei number. The phase plot is divided in to five different regimes with well-defined boundaries based on the shape

and path of the bubble. The Galilei number Ga is mentioned in the X-axis which ranges from 7 to 500, and it is Eotvos number Eo in the Y-axis which ranges from 0.1 to 200. The bubbles are axisymmetric in regime I, non-axisymmetric in regime II and III, and the bubbles breaks in regime IV and V.
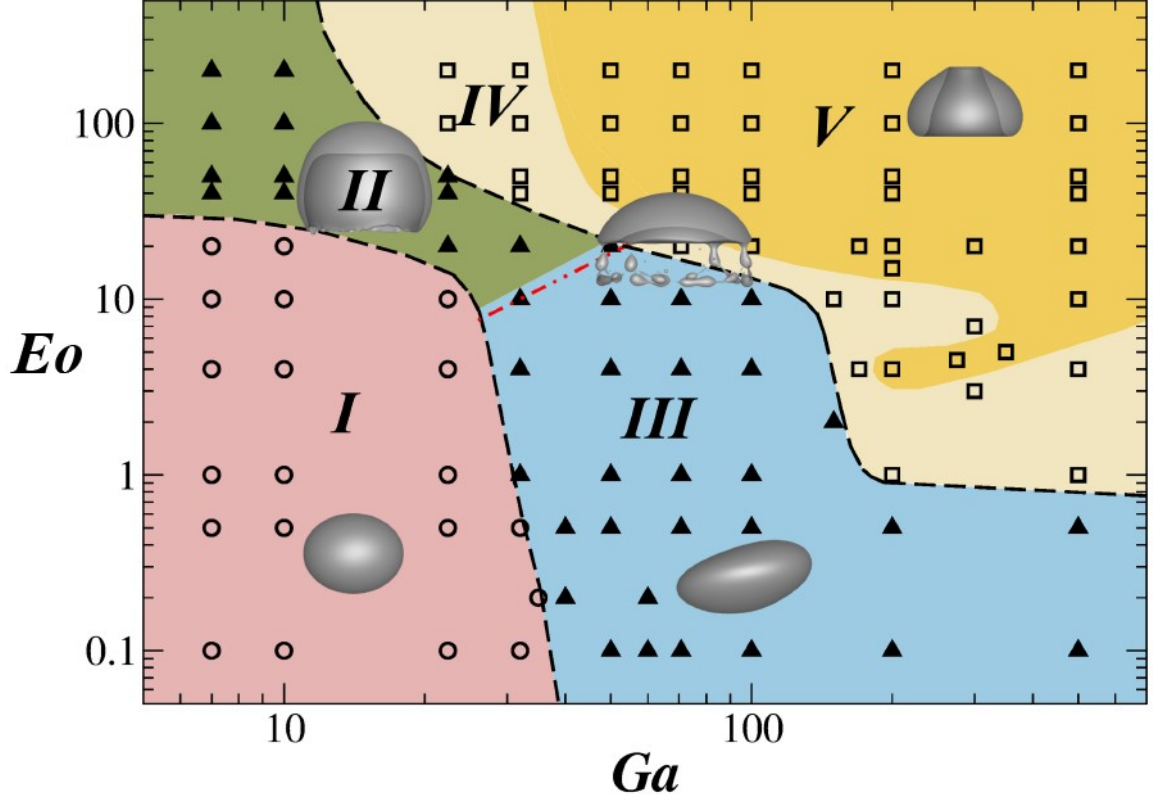
Figure 2.1: Five different regimes on the Eo-Ga phase plot. Figure taken from Tripathi et al [2] with permission. © NATURE PUBLISHING GROUP.

Regime I corresponds to low Eotvos and Galilei numbers. This indicates the surface tension value is relatively higher and the effect of gravity is low. The bubbles in this regime are spherical or ellipsoidal in shape. The bubble rises vertically upwards at its terminal velocity without any path oscillation and maintains its axisymmetric nature throughout its motion. Regime II has high Eotvos and low Galilei numbers. The bubbles belonging to this regime show an axisymmetric cap shape with a thin skirt trailing the main body of the bubble. This thin skirt part moves in the form of waves and doesn't show axisymmetric nature, which makes the bubble as asymmetric in shape. The bubbles in this regime rise vertically upwards without any oscillation in path. Regime III occupies lower Eotvos and higher Galilei number. Here both surface tension and inertia force are equally significant. The bubbles is not axisymmetric in this regime with continuous variation in shape and rises in a zigzag or spiral manner. In regime IV and regime V, the effect of gravity is higher with relatively weak surface tension. So the bubble breaks up and undergoes a change in shape. Before the break up the bubble follows an axisymmetric nature. The bubble in regime IV breaks into a large axisymmetric spherical cap with small satellite bubbles in its caps wake, and this kind of breakup is referred as peripheral breakup. Such a bubble regains its axisymmetry after the breakup

and it rises upwards with a terminal velocity. The regime V bubble shows some different kind of dynamics. A dimple formation in the bottom center of the bubble leads to change in its shape to doughnut-like or toroidal shape with the ejection of small satellite bubbles. But at higher value of Eo and Ga a perfectly axisymmetric change in shape of the whole bubble is observed without any satellite bubbles. This toroidal shape is not permanent. It eventually loses symmetry and breaks up into multiple fragments.

We have already discussed about Morton number $Mo = Eo^3/Ga^4$. This Morton number is independent of the size of the bubble and it depends only on the physical properties of the fluid. So Morton number can be represented as a straight line with an inclination in the Eotvos Galilei phase plot. For every fluid at similar surrounding condition it will have a constant Morton number value. So constant Morton number line in the Eo - Ga phase plot indicates a particular fluid with density ρ, surface tension σ, and viscosity μ. Tripathi et al [2]. conducted numerical simulation for a rising gas bubble in different fluids. And these fluids are indicated in the phase plot as constant Morton number lines.
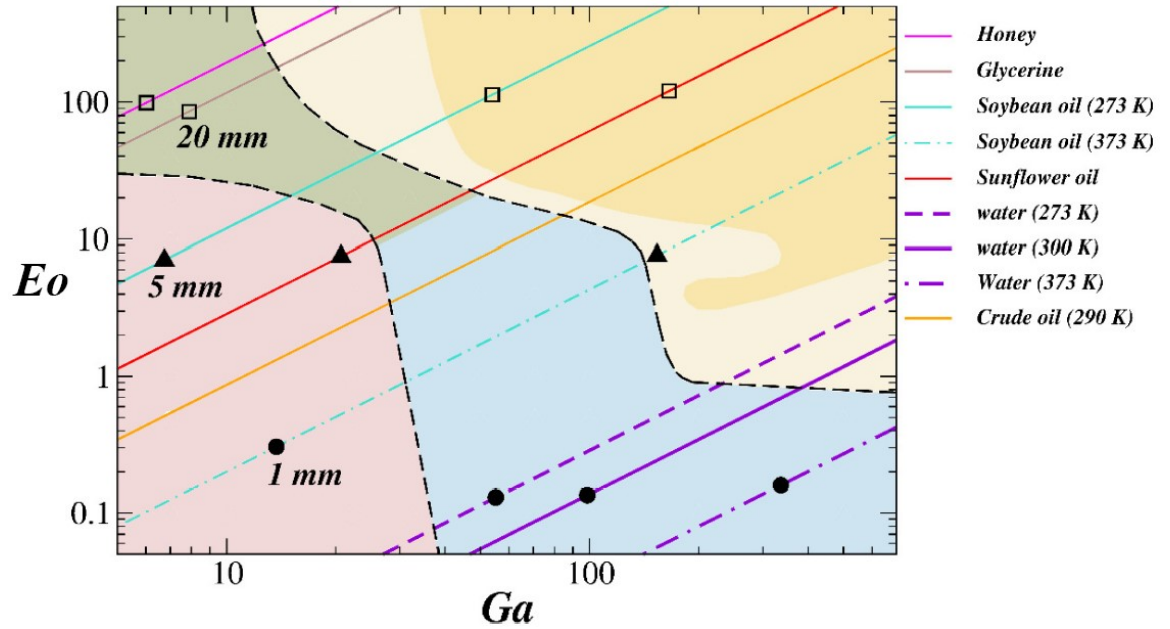
Figure 2.2: Eo-Ga phase plot with constant Morton number lines. Figure taken from Tripathi et al [2] with permission. © NATURE PUBLISHING GROUP.

The air bubble at a particular fluid at a particular temperature will lie on constant Morton number lines. So as the size of the bubble increases, the position of the bubble in the Eo-Ga phase plot rises along the constant Morton number line corresponding to that particular fluid. The extreme Morton number which is corresponding to honey is $Mo = 678$, and for water at 373 K is $Mo = 2.9 \times 10^{-11}$. All the other fluids which are mentioned in the figure will have the Morton numbers lying between these two values.

Consider the case of soya bean oil at 273 K with Morton number = 0.16. The bubble of radius 5 mm in it will show an ellipsoidal shape and rise vertically upwards which is clearly in regime I. As the bubble size is increased it becomes a skirted bubble (regime II) and further increase in size say around 20 mm radius the toroidal shaped bubbles are formed (regime V). Similar kind of behavior

is observed for all the fluids. So by knowing the properties of the fluid and the size of the bubble, it is possible to predict its nature very easily.

The regime II and regime III are separated by a constant Morton number line with $Mo = 10^{-3}$. Below this line the spiraling and zigzagging trajectory of the rising bubble is observed. In some earlier studies as described by Ryskin and Leal [17] the path instability occurs due to vortex shedding from the bubble. The asymmetry in planar forces because of this vortex shedding results in shape asymmetry. Similarly any asymmetry of shape in a horizontal plane results in the imbalance of forces, which leads to path oscillation of the bubble.

Till now we discussed about the numerical simulation results of a gas bubble rising in fluids of different viscosity. In the coming chapter we will explain about an experimental setup and our methodologies in order to replicate the Eotvos-Galilei phase plot.

Chapter 3

Experimental Setup and Methodology

The experimental setup as shown in Figure 3.1, consists of (i) an acrylic test tank (ii) nozzle connected to a syringe (iii) dumping cup mechanism and (iv) a high-speed camera along with back lighting and a computer. This enabled us to visualize air bubbles of different sizes rising in a transparent tank by means of a high speed camera system.

Figure 3.1: Schematic diagram of the experimental setup

The tank is made of transparent acrylic with cross section of 200 X 200 mm and 700 mm depth with a wall thickness of 8 mm. These dimensions are good enough for the air bubbles rising in viscous fluid to visualize without any disturbances. During the experiments t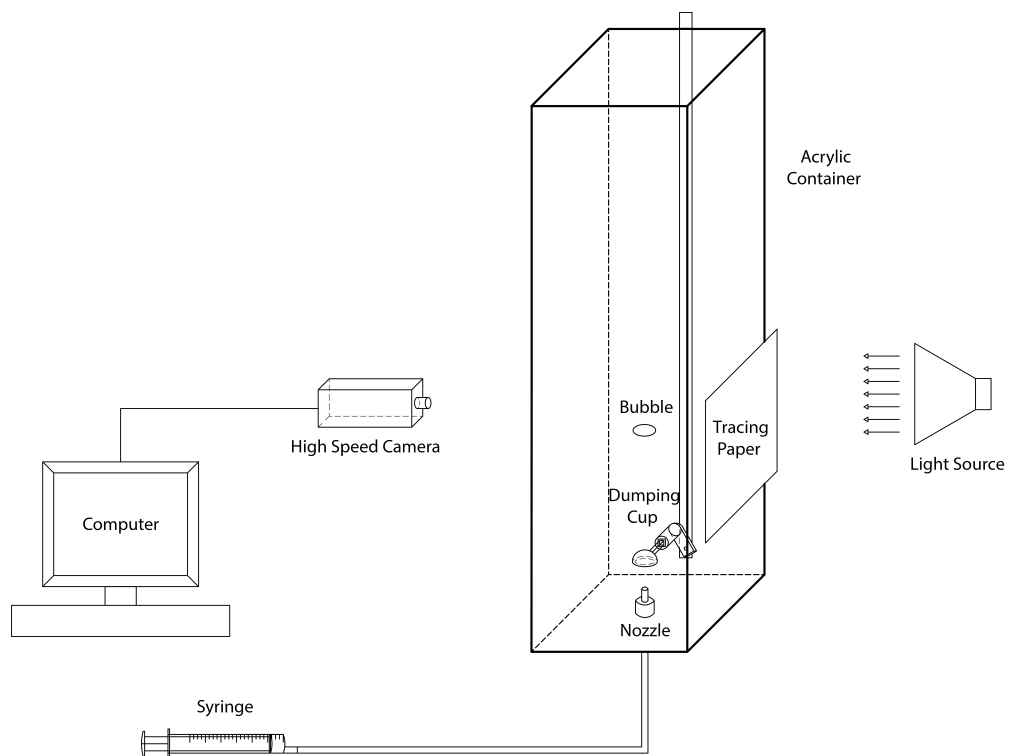he fluid was filled inside the acrylic tank and is kept at a constant height of 300 mm (from bottom) for all experiments.

The stainless steel nozzle with a flat opening was installed at the center of the bottom of the tank. The upper surface of the nozzle was kept at 30 mm from the bottom of the tank to avoid the bottom wall interactions. The nozzle is connected to a typical plastic medical syringe through a PTFE (Poly Tetra Fluoro Ethylene) tubing. The bubbles are created by pushing the plunger of the syringe which is filled with air initially. This air enters the bottom of fluid medium through the nozzle. The bubbles created by the nozzle are small spherical and almost consistent in size. The radius of the bubble was estimated to be 1.37 mm based on the front view image and from the pixel to mm calibration.

For getting bubbles of larger sizes a dumping cup mechanism is used. The dumping cup mechanism consists of three components - (i) one cup shaped part with a hemispherical dome in the end (Figure 3.2(b)), (ii) a holder (Figure 3.2(a)) which is connected to the bottom wall of the tank through a ball bearing and (iii) a rod (not shown in Figure) connected to one end of the holder for rotating the cup. The cup has a square cross-sectional projection which can be inserted into the hollow like structure of the holder. The holder is designed such that dumping cup of different sizes (diameter) can be connected to it. These parts were drawn in SOLID EDGE and are fabricated using a 3D printer (uPrint SE by Stratasys). The role of the rod is to turn the dumping cup after it is filled with air to release all the air at one time as a single bubble. An angle of rotation of 150 degree is possible with this arrangement. In its initial position the dumping cup is placed right above the nozzle and a calibrated volume of air is injected through the nozzle and gets collected inside the dumping cup. Although the individual bubbles from the nozzle are small (1.37 mm) when they are collected inside the dumping cup they coalesce together to form a larger mass of air. When the dumping cup is turned with the rod this air is released and it rises as a single bubble. The radius of released bubble is calculated as radius of a sphere having a volume equivalent to the volume collected under the dumping cup. This volume is known because we injected a known volume of air through the syringe.
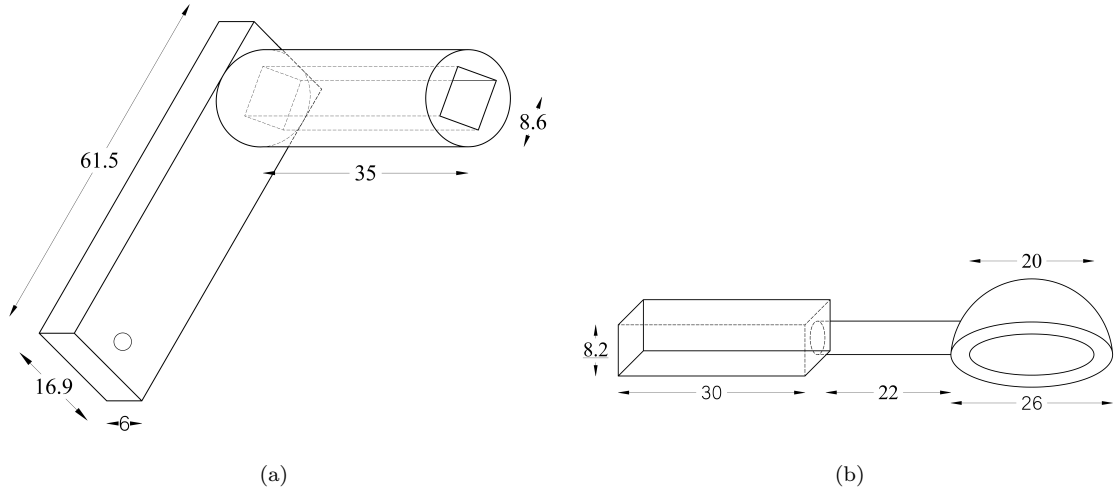
Figure 3.2: Components of Dumping Cup (a) Holder, (b) cup

Bubble visualization - Almost all the experimental techniques in bubble dynamics uses the differences in refractive indices of water and air to visualize the bubble. In our setup the bubbles are recorded by using the high-speed camera (Photron FASTCAM SA1.1) as shown in Figure 3.3 which is capable of capturing 675000 fps at reduced resolutions. In these experiments a resolution of 448×800 pixels, a frame rate of 3000 fps and an exposure time of 1/3000s was used. This camera is connected to a computer with Photron FASTCAM Viewer (PFV, Figure 3.4) application installed in it through LAN port. The camera can be controlled by using this PFV software. Two LED lighting systems along with the controller (Videoflood Controller by Visual Instrumentation Corporations) were installed opposite to the camera and provide illumination using a diffused backlighting method (using a tracing paper). This diffuse backlighting illumination allows a clear visualization of the bubble boundaries on a light background.

Figure 3.3: Photron FASTCAM SA1.1 High Speed Camera

We conducted our preliminary experiments with pure water as the fluid medium. Since viscosity and surface tension terms are of great importance in these experiments, ultra pure Millipore water with a purity of $18.2 M\Omega$ was chosen over a normal tap water to avoid the impurities. This also ensures the same quality of water in all the experiments. The air is sucked in to the syringe and is

14

connected to the nozzle. The syringe plunger is pressed carefully for releasing the bubble through the nozzle. And the bubble is captured using a high-speed camera. In order to obtain dimensions of the bubble, calibration of the camera has to be done. This is done by capturing a graduated scale which is kept exactly in the same plane of the nozzle and perfectly vertical. From the image of graduated scale the pixel to mm conversion can be obtained.
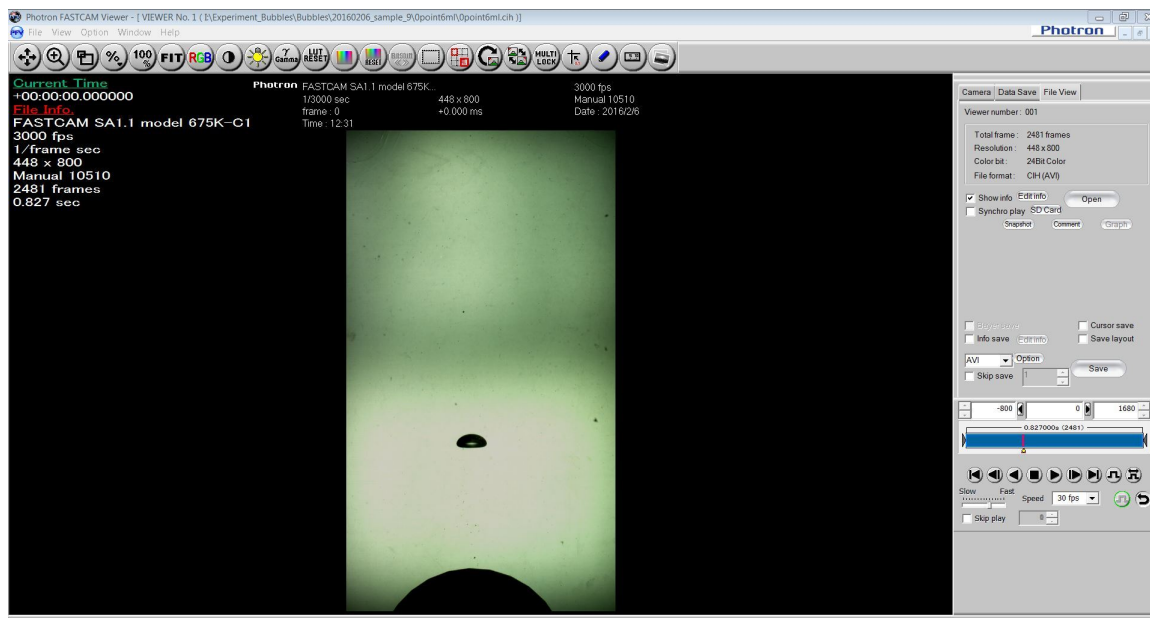
Figure 3.4: Photron FASTCAM Viewer application

The Millipore water at room temperature has a Morton number of 2.86×10^{-11}. This corresponds to a single straight line in the Eo-Ga phase plot. By changing the size of the bubble, we got few points along this straight line. The smaller bubbles were oscillatory in nature with asymmetric shape. And the larger ones showed peripheral breakup. This clearly indicated these bubbles lie in Regime III and Regime IV respectively. In order to get the bubbles in other regimes the fluid medium needs to be changed. The fluid media like honey, crude oil, sunflower oil, and soybean oil as described in the Eo-Ga phase plot of Figure 2.2 are not practical to use for the experiments because of their opaque nature and high cost. For the bubble to be clearly visible during video capturing, the fluid medium should be very transparent. So the only alternative is to choose some other fluids which have viscosity, surface tension and density similar to the aforementioned fluids and with transparency good enough to capture the bubble clearly.

Aqueous glycerol solutions of different concentrations were chosen to change the Morton number of the fluid medium. The concentration of aqueous glycerol solution are varied by mixing it with Millipore water carefully, and the solution is allowed to rest for few hours for thorough mixing. This glycerol solution is a well-known Newtonian fluid with very good transparency and its viscosity can be varied from 1660 cP to 1 cP by changing its concentration. So with the help of aqueous glycerol solutions it is possible to get almost all the points between constant Morton number lines corresponding to glycerol and pure water. Hence we decided to choose this aqueous glycerol solutions for our further experiments.

We used the MCR 301 Rheometer by Anton Paar for checking the viscosity. With this rheometer

it is possible to measure the viscosity after bringing the sample to any particular temperature and with variable shear rate. Before checking the viscosity, temperature of the measuring surface of rheometer was brought to 303 K, the room temperature at which the experiments are being conducted. A highest value of dynamic viscosity of 1657 cP was noted for 100% glycerol and the lowest value of 1 cP for pure water.

The experiments on rising gas bubble has been conducted in 18 different aqueous glycerol solutions and with pure Millipore water. As compared to viscosity, the variation in surface tension and density of these solutions were relatively small. So we took those physical properties from standard articles [18]. The viscosity, surface tension, density and the corresponding Morton number values of all these samples are tabulated in Table 3.1.

Table 3.1: Properties of different samples

Sample No.	% of Glycerol	Viscosity	Density	Surface tension	Morton Number
1	100	1657	1260	0.06208	230.314
2	99.8	1524	1259	0.06219	163.38
3	98.2	1115	1256	0.06228	46.48
4	97.1	967.8	1254	0.06239	28.259
5	95.9	797	1249	0.06263	12.9
6	94.8	681	1246	0.06282	6.83
7	93.7	581	1243	0.06298	3.6
8	92.2	478	1241	0.06309	1.6
9	90.8	319.7	1235	0.0634	0.3256
10	88.5	258	1230	0.0636	0.1372
11	85	170	1222	0.0642	0.0253
12	80	96.9	1209	0.06478	0.00263
13	70	57.75	1182	0.06578	0.000324
14	60	26	1154	0.06663	1.315×10^{-5}
15	50	15.1	1127	0.0675	1.5×10^{-6}
16	40	9.6	1100	0.0684	2.4×10^{-7}
17	25	7	1061	0.06949	6.57×10^{-8}
18	10	4.3	1023	0.06978	9.56×10^{-9}
19	Pure water	1	1000	0.073	2.52×10^{-11}

3.1 Experimental Procedure

- The first step of this experiment is filling the acrylic test tank with fluid medium to a depth of 300 mm.

- Fix the High-speed camera on tripod and face its lens part towards one wall of the tank. Make sure that, line of sight of camera and the side wall of the tank are mutually perpendicular to each other.

- Install the back light illumination system.

- Connect the camera to the computer and switch on the power supply.

- Adjust the position of the camera so that the dumping cup part is visible in the screen exactly at the middle.

- In order to get the lighting and focus, the aperture of the lens is adjusted.

- Focus the lens on the dumping cup in order to get clear boundary of it, which is in the same plane where the bubbles are rising.

- Calibration of the camera is done by capturing a graduated scale which is kept perfectly vertical over the dumping cup.

- The bubbles are created by injecting quantified volume of air through the nozzle by means of a syringe. By knowing the volume, equivalent radius of the bubble can be obtained from the volume of sphere formula. Bubbles with volume 0.2, 0.4, 0.6, 1, 2, 5, 10, 16, 20, 30, 50, 60, 70 and 80 ml are created in all the samples with corresponding equivalent radius ranges from 3.62 mm to 26.7 mm.

The recorded images were saved to the computer in AVI format. After clearly examining the image files each bubble is classified in to different regimes based on its shape and path behavior. Even though the images that we got were in focus, there were lots of obstructions in the form of tiny bubbles in the vicinity of the rising bubble. These tiny bubbles were removed from the image with the help of MATLAB based image processing tool. For this image processing a particular frame of the image is given as the input. This image is cropped into a resolution of 796×446. Then the cropped color image is converted into a gray scale image with *rbg2gray()* command. The gray scale image is filtered with a median filter command to get a final filtered image which is free from these background particles.

Chapter 4

Results and Discussion

We have conducted around 297 experiments of gas bubble rising in aqueous glycerol solutions of 18 different concentrations and in pure Millipore water. By selecting these fluids we changed the Morton number from 230 (Pure Glycerol) all the way to 2.52×10^{-11} (Pure Water). This helped us to cover almost entire area of the Ga-Eo phase plot as in Figure 2.1. In each glycerol sample we created an average of 16 different sized bubbles with radius varying from 3.6 mm to 26.7 mm with the help of the dumping cup mechanism. The images of these bubbles' captured by the high-speed camera were examined thoroughly, and are plotted in Eo-Ga plane. After verifying the path and shape of each bubble clear solid lines are drawn in the phase plot which divides it into four different regimes. The phase plot that we constructed through our experimental result is shown in Figure 4.1.

Through our experimental study we succeeded to replicate the Galilei-Eotvos phase plot of a gas bubble rising in viscous fluids. But this phase plot is slightly different from the one obtained through numerical simulation by Tripathi et al (Figure 2.1). The first important thing we noticed is that unlike five different regimes in the phase plot as in Figure 2.1 here there are only four regimes. We could not get a single bubble with a toroidal breakup which is in the regime V of the Figure 2.1. It is because of the initial condition of the gas bubble. In the numerical simulation by Tripathi et al [2]. for all cases they kept the initial shape of bubble as spherical. But in our case we could not keep bubble shape as spherical for larger bubble. Practically it is impossible to keep a large bubble into exact spherical initial shape, because for larger bubble the inertia force is very high compared to surface tension. The regime V of the numerical simulation (Figure 2.1) consist of bubbles with a high value of Ga and Eo numbers, which implies a larger inertia force and relatively lower surface tension. This low surface tension force is not enough to keep larger bubbles into exactly spherical shape. Also the viscosity ratio and density ratio were kept constant in all of the simulation by Tripathi et al. [2]. They chose density ratio $\rho_r = 10^{-3}$ and viscosity ratio, $\mu_r = 10^{-2}$. These values corresponds to air water system. But in our experiments we used 19 different samples with different viscosity and density values. So each Morton number line in the phase plot corresponds to a particular value of density ratio and viscosity ratio.
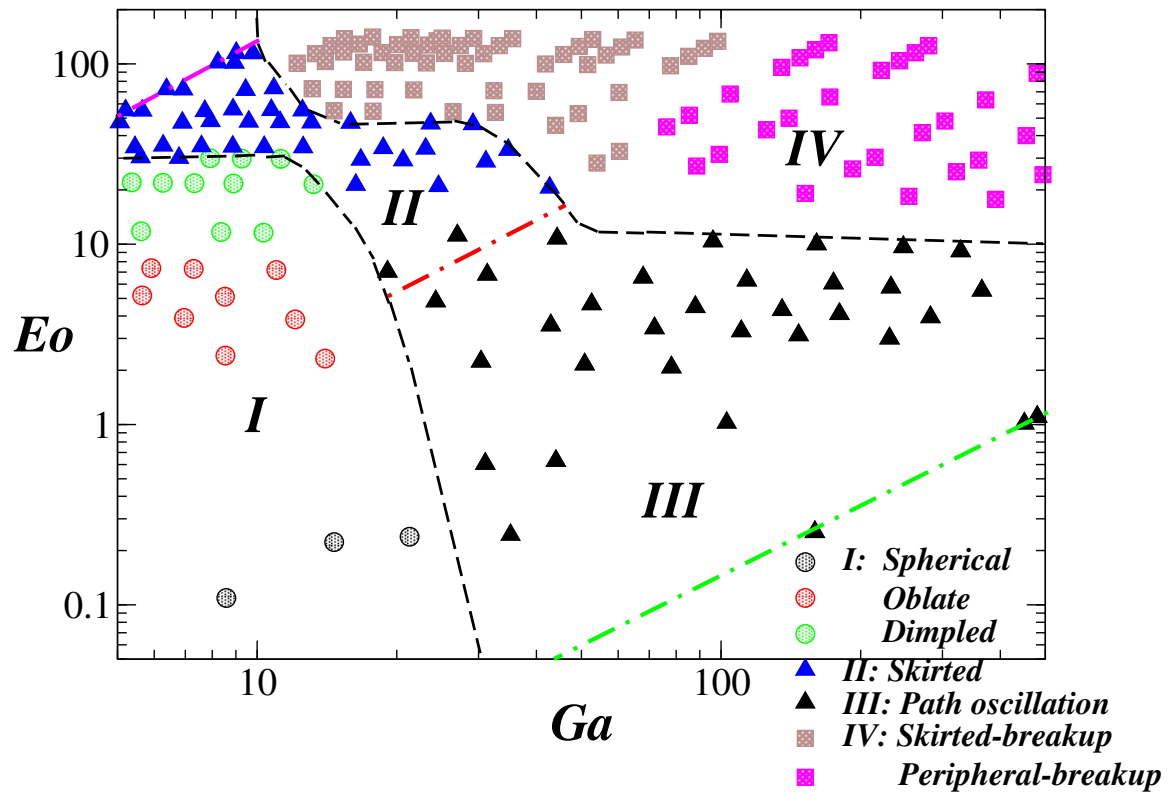
Figure 4.1: Different regimes of bubble shape and behavior based on Experimental results; Circles, solid triangles and squares represent the axisymmetric (regime 1), asymmetric and breakup regimes, respectively. The asymmetric region is further classiffed into two regimes: non-oscillatory regime (regime II) and oscillatory regime (regime III). Regime IV consist of two kind of breakup. Skirted breakup and Peripheral breakup. The red dash-dotted line is the $Mo = 10^{-3}$. line separates region II and region III as observed by [2]

.

Now we would like to discuss about each regime in detail. We classified the bubble with axisymmetric shape as regime I. This bubble rises vertically upwards without any oscillations. Regime I bubble has low Eotvos and Galilei numbers. This indicates low inertia force and relatively high surface tension acting on the bubble. So the bubbles are spherical in shape. An example for spherical bubble is shown in Figure 4.2(a). As the Eotvos number increases within this regime the bubbles cannot remain as spherical because of low surface tension and they form an oblate spherical shape (Figure 4.3(a)). But it is very hard to distinguish between oblate and spherical bubble. If the diameter of the bubble in two perpendicular direction differ by $2 \times mm$ per pixel, we classified them as oblate spherical bubbles. Disc shaped bubbles (Figure 1.1(b)) also come under oblate spherical bubble. At even higher Eotvos number we found a small dimple like depression formed at the bottom of the bubble, and named it as dimple shaped bubble (Figure 4.5). These kind of bubbles have sharp edges in the bottom. Dimple shaped bubbles were observed near the boundary of regime II.

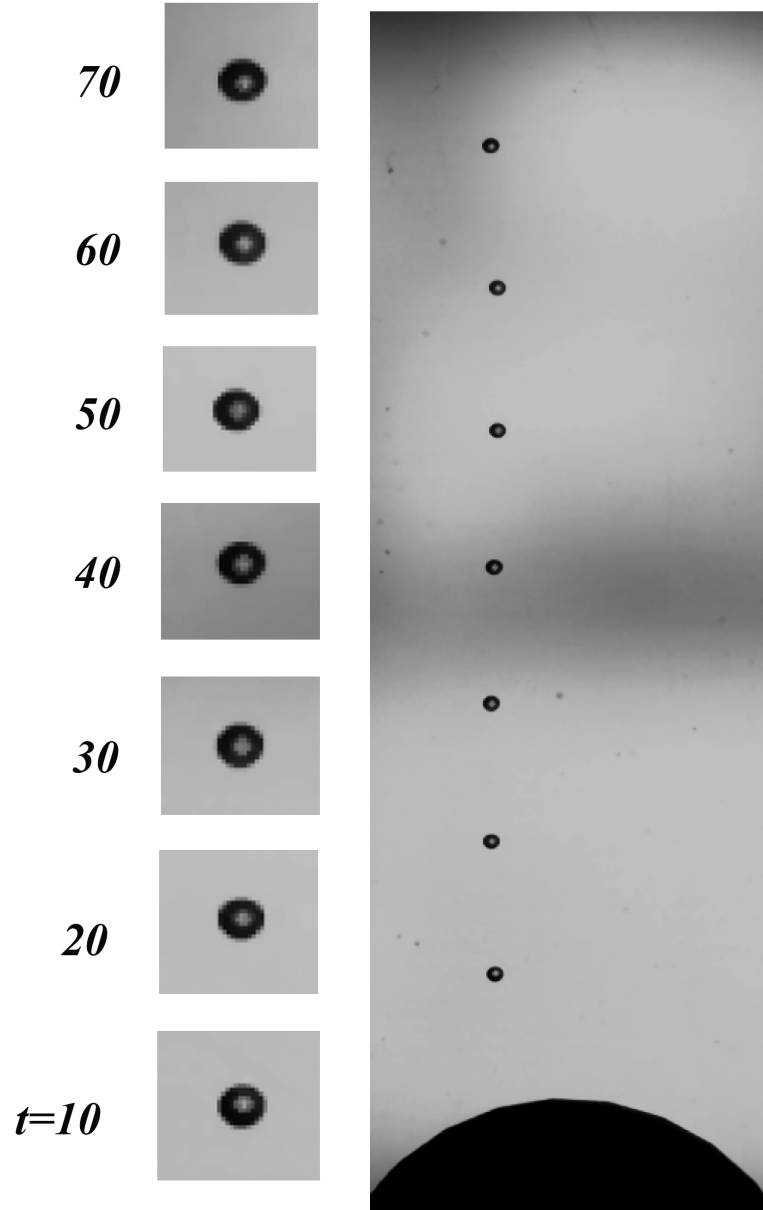Figure 4.2: Evolution of shape of regime I bubble (Spherical shape): 25% of glycerol in water, $\mu_r = 1.43 \times 10^{-3}$, $\rho_r = 9.4 \times 10^{-4}$, $R = 12.6$ mm, $Ga = 21.3$ and $Eo = 0.238$
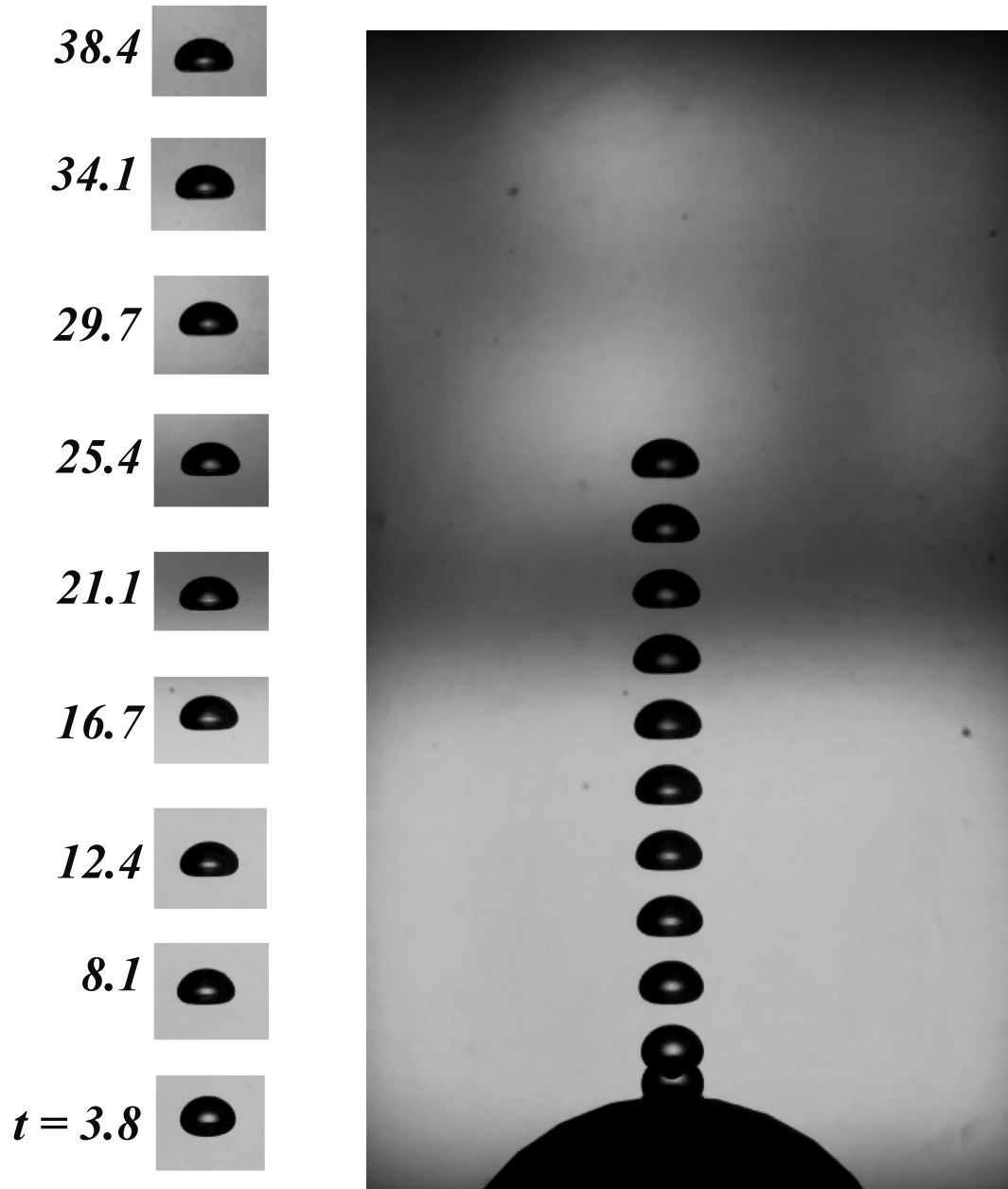
Figure 4.3: Evolution of shape of regime I bubble (Oblate shape): 94.8% of glycerol in water, $\mu_r = 1.47 \times 10^{-5}$, $\rho_r = 8.03 \times 10^{-4}$, $R = 5.2$ mm, $Ga = 2.17$ and $Eo = 5.33$

Figure 4.4: Evolution of shape of regime I bubble (Disc shape): 80% of glycerol in water, $\mu_r = 1.03 \times 10^{-4}$, $\rho_r = 8.3 \times 10^{-4}$, $R = 3.6$ mm, $Ga = 8.5$ and $Eo = 2.4$

14.0
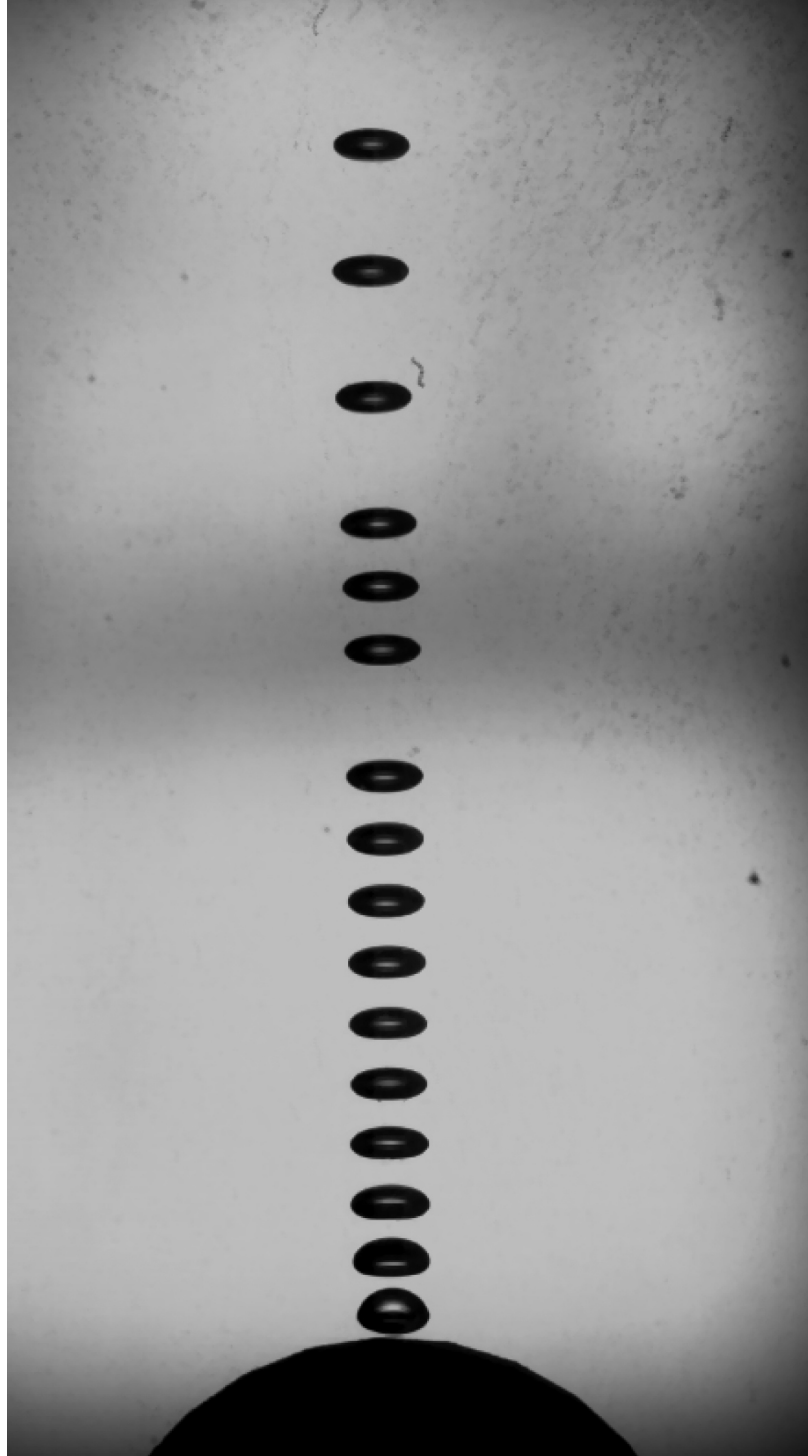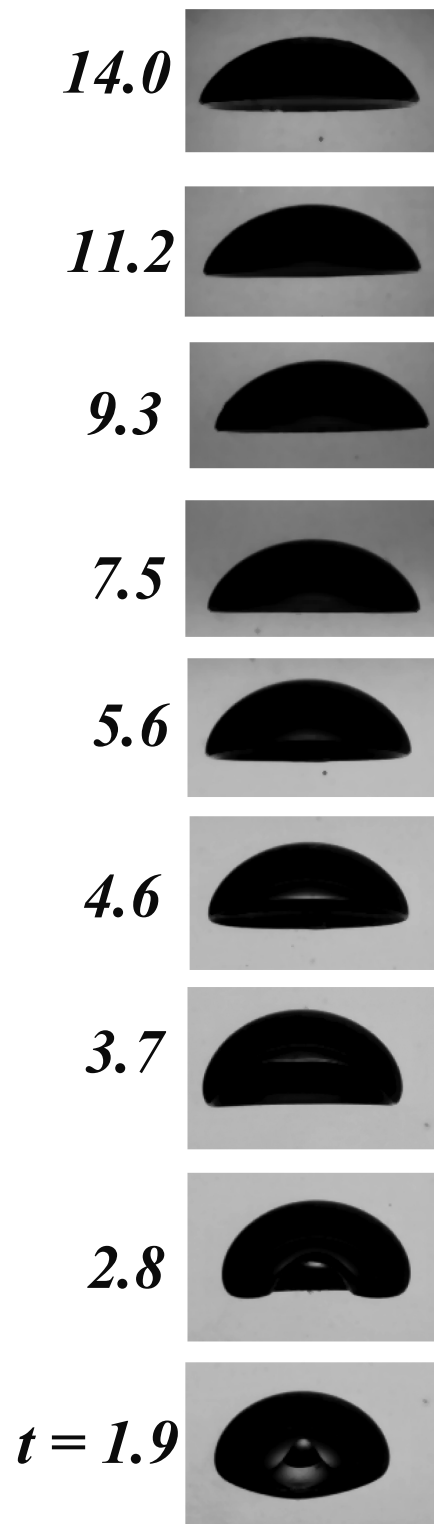
11.2

9.3

7.5

5.6

4.6

3.7

2.8

$t = 1.9$

Figure 4.5: Evolution of shape of regime I bubble (Dimple shape): 92.2% of glycerol in water, $\mu_r = 2.09 \times 10^{-5}$, $\rho_r = 8.05 \times 10^{-4}$, $R = 12.4$ mm, $Ga = 11.2$ and $Eo = 29.7$

In these images evolution of a single bubble with time is presented. The time mentioned here is the non-dimensional time.

$$\text{Non} - \text{dimensional time}, \text{t}^* = t\sqrt{\frac{9.81}{R}} = \frac{frame}{frame \; per \; second}\sqrt{\frac{9.81}{R}} \tag{4.1}$$

It is clear that, the shapes of bubble in regime I, such as spherical, oblate spherical or dimple shaped maintains its constant shape throughout its motion and is rising vertically upwards without any path oscillation. We could not get more bubble with spherical shape in regime I. These spherical bubbles are of very small in size with radius around 2 mm. It is very hard to create bubbles of even smaller size with our setup since the fluid medium is high viscous glycerol solution.

The bubble in regime II shows an axisymmetric cap shape with a thin skirt trailing the main body of the bubble and rises vertically upwards without any path oscillations. This thin skirt part moves in the form of waves and does not show axisymmetric nature, which makes the bubble as asymmetric in shape. a skirt shaped bubble is shown in Figure 4.6(a). These bubbles were observed only in high viscous glycerol solutions with medium sized bubble. In our experiments we found bubble with skirt in all samples of glycerol solution from 80% by volume to pure glycerol. This regime has low Galilei number and higher Eotvos number. Because of low surface tension of the fluid, bubble cannot possess a spherical shape and edges of a dimple shaped bubble elongate to form a thin skirt. This shape is very unstable and a further increase in size of bubble leads to breakup of this skirt in to small bubble fragments.
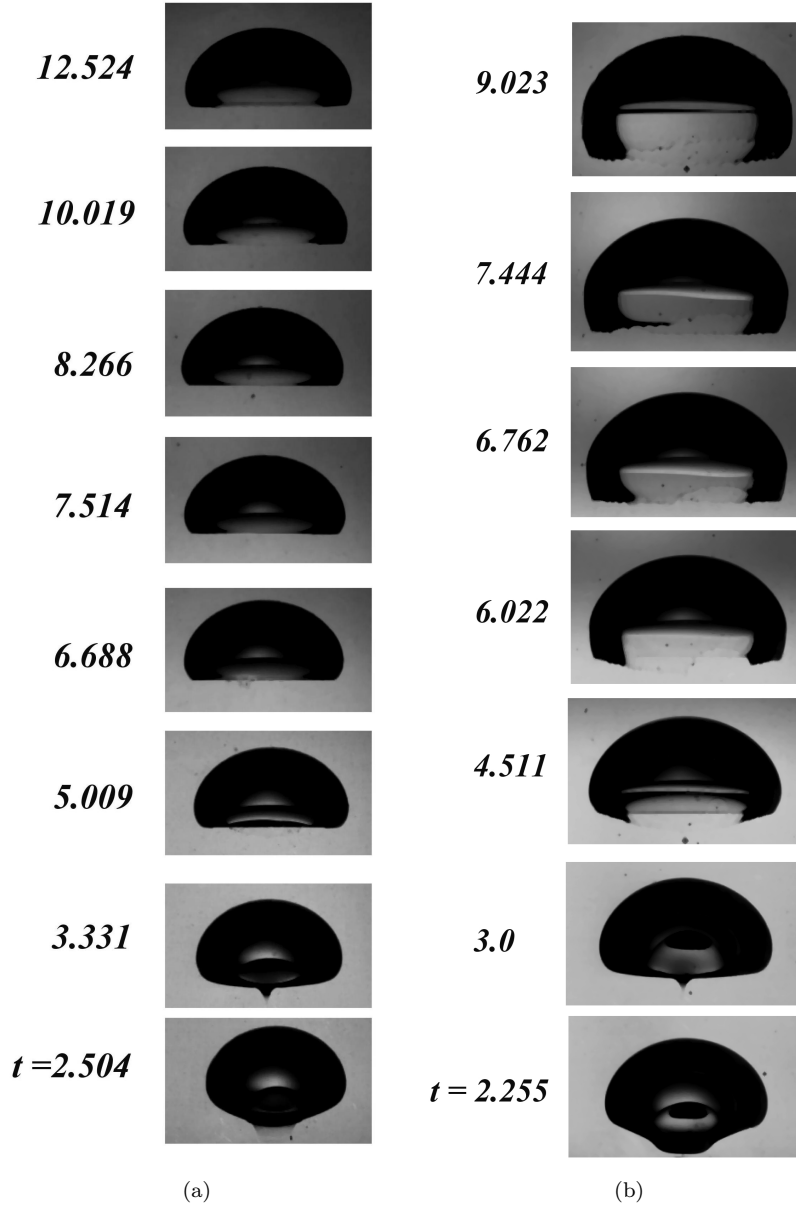
Figure 4.6: Evolution of shape of regime II bubble (Skirt shape): (a) 99.8% of glycerol in water, $\mu_r = 6.56 \times 10^{-6}$, $\rho_r = 7.9 \times 10^{-4}$, $R = 15.6$ mm, $Ga = 5.05$ and $Eo = 47.46$; (b) 98.2% of glycerol in water, $\mu_r = 8.96 \times 10^{-6}$, $\rho_r = 7.96 \times 10^{-4}$, $R = 19.3$ mm, $Ga = 9.44$ and $Eo = 71.78$

The above mentioned images are skirt shaped and it belongs to regime II. In fact these bubbles are axisymmetric spherical cap shape but a very thin skirt like structure is trailing the main body of the bubble. This skirt part possesses a wave like motion which makes the bubble asymmetric in shape. This kind of bubble follows a vertical path without any oscillation.

The regime III bubbles are asymmetric in shape which varies continuously as it rises and show path oscillation. These kind of behavior was observed with smaller sized bubble rising in water at low viscous glycerol solutions. Bubbles in this regime occupy low Eotvos and high Galilei number. Here both surface tension and inertia force are equally significant. Because of that bubble remain integral throughout its motion. A constant Morton number line of 10^{-3} separates regime III with regime II. As compared to the Ga-Eo phase plot through numerical simulation (Figure 2.1), here the regime III is slightly broader towards high Galilei number side. It is because of initial condition of the bubble. In numerical simulation Tripathi et al. considered the bubble as initially spherical in all cases. But in these fluids it is practically impossible to keep bubble of larger size in spherical shape due to its low surface tension.
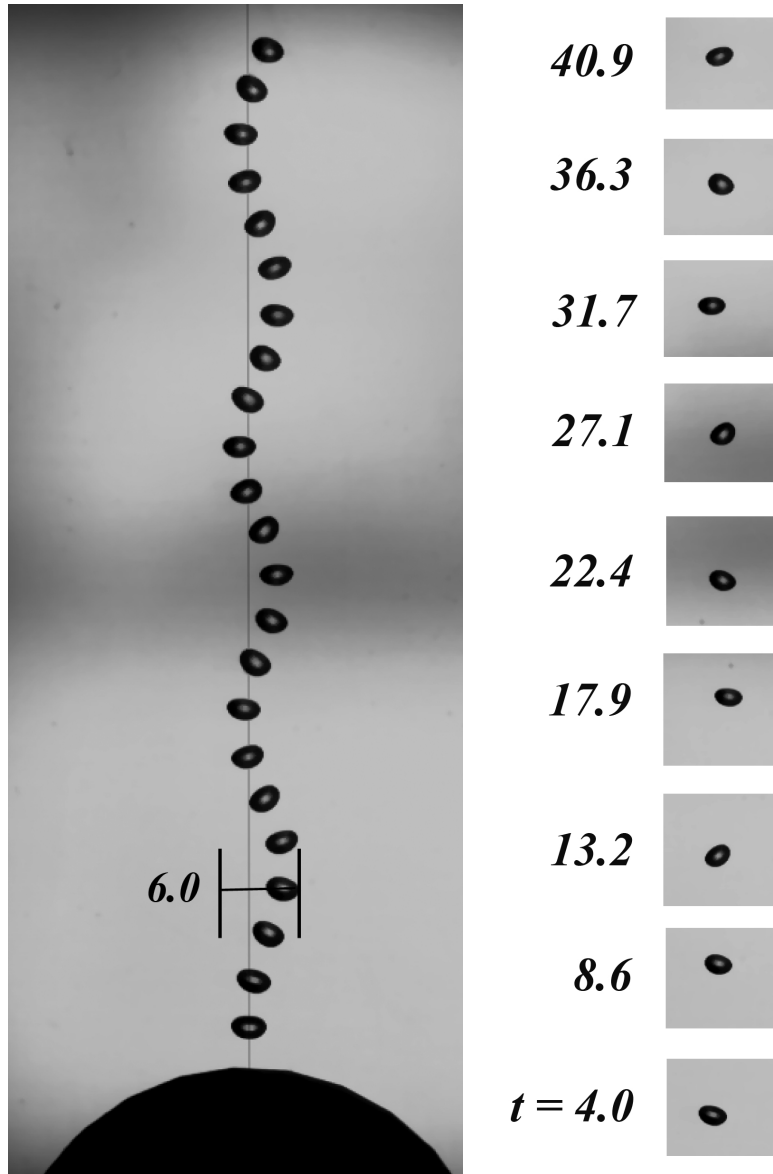
Figure 4.7: Evolution of shape of regime III bubble: 25% of glycerol in water, $\mu_r = 1.43 \times 10^{-3}$, $\rho_r = 9.4 \times 10^{-4}$, $R = 2.04$ mm, $Ga = 44.06$ and $Eo = 0.628$
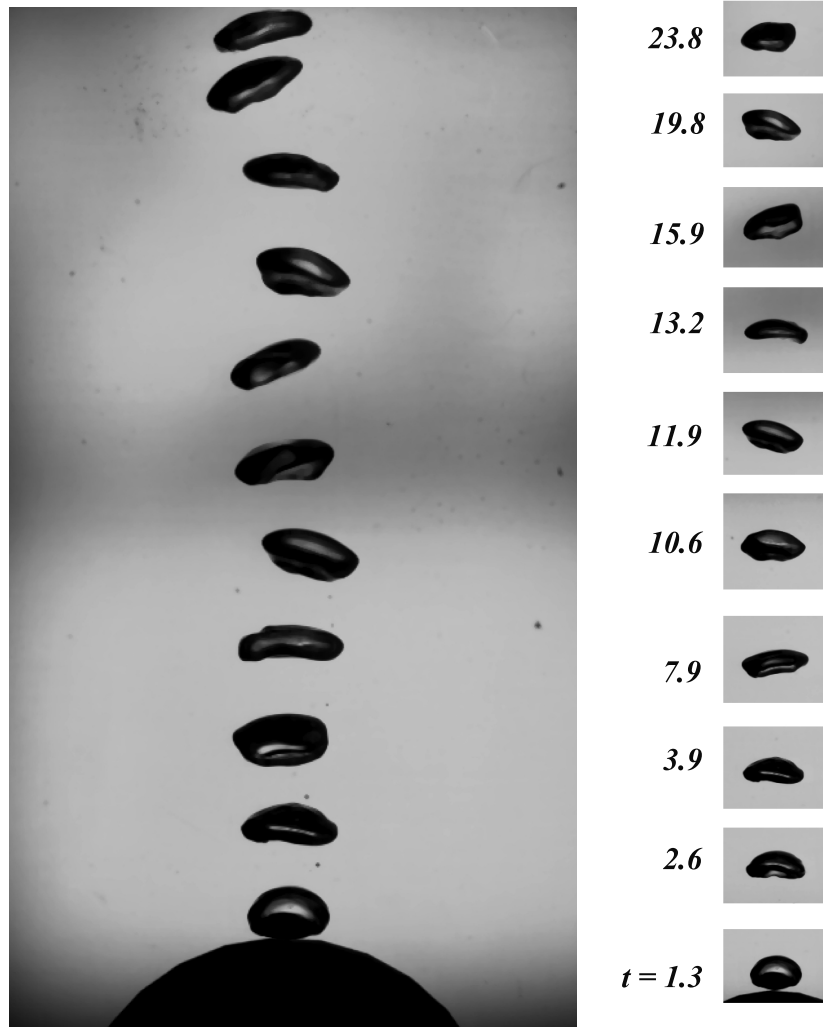
Figure 4.8: Evolution of shape of regime III bubble : 10% of glycerol in water, $\mu_r = 2.33 \times 10^{-3}$, $\rho_r = 9.77 \times 10^{-4}$, $R = 6.2$ mm, $Ga = 364.93$ and $Eo = 5.53$

From Figure 4.7(a) we can see that bubble is oscillating as it rises. For this bubble the extent of oscillation was found to be six times its radius. Also its shape is changing continuously as it rises, which makes the bubble asymmetric in shape. Similar kind of behavior is observed for all regime III bubble.

The breakup bubbles observed in our experiments are characterized as regime IV. Two types of breakup were seen here. Skirted breakup (Figure 4.9, 4.10) and peripheral breakup (Figure 4.11, 4.12, 4.13). Skirted breakup bubbles are observed near to boundary of regime II and peripheral breakup near to boundary of regime III. Even though we observed two different kind of breakup in regime IV, it is very hard to distinguish between them. Before the breakup the bubble in this regime possesses a skirt shape or an oblate spherical shape. Those two shape was asymmetric but some close symmetry was observed. Regime IV occupies high Galilei and Eotvos number, which means the inertia force is very large with weak surface tension effect. So bubble become very unstable in its shape and it breaks up and undergoes change in shape. In skirted breakup, thin skirt of the bubble detaches from its main body to form a large axisymmetric spherical cap and multiple tiny bubble fragments in its cap's wake. In peripheral breakup the large oblate spherical shaped bubble breaks to form an asymmetric spherical cap with small satellite bubbles in its cap's wake. So briefly a skirted breakup result in an axisymmetric spherical cap, while through peripheral breakup asymmetric spherical cap shaped bubbles are formed.

8.036

7.240

6.443

5.623

4.826

4.030

3.209

t = 1.167

Figure 4.9: Evolution of shape of regime IV bubble (Skirt breakup): 93.7% of glycerol in water, $\mu_r = 1.72 \times 10^{-5}$, $\rho_r = 8.04 \times 10^{-4}$, $R = 16.84$ mm, $Ga = 14.64$ and $Eo = 54.91$

9.023

7.511
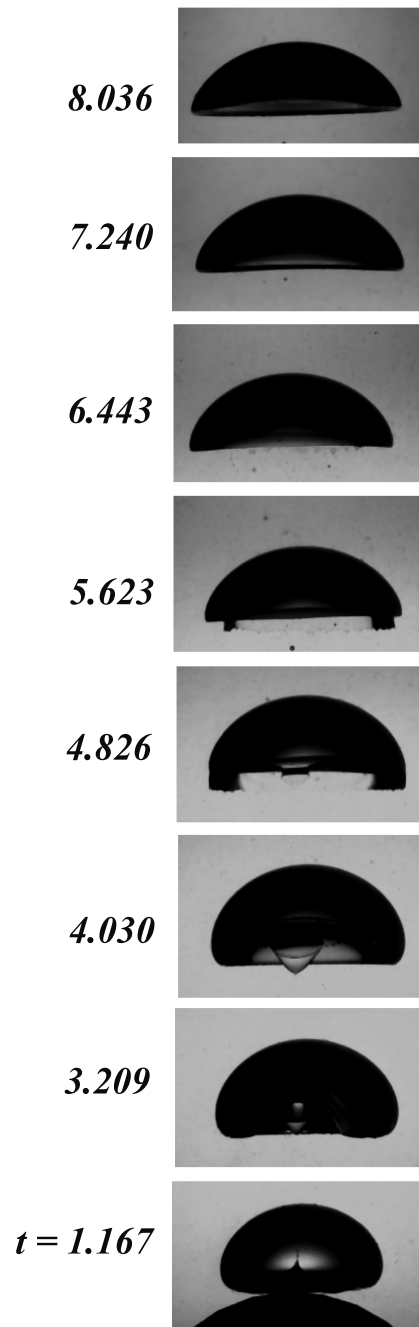
6.022

4.511

3.0

t = 1.511

Figure 4.10: Evolution of shape of regime IV bubble (Skirt breakup): 94.8% of glycerol in water, $\mu_r = 1.47 \times 10^{-5}$, $\rho_r = 8.02 \times 10^{-4}$, $R = 19.27$ mm, $Ga = 15.34$ and $Eo = 72.32$

7.662

6.378

5.114

3.831

t = 2.547

Figure 4.11: Evolution of shape of regime IV bubble (Peripheral breakup): 70% of glycerol in water, $\mu_r = 1.73 \times 10^{-4}$, $\rho_r = 8.46 \times 10^{-4}$, $R = 26.7$ mm, $Ga = 280.22$ and $Eo = 126$

8.038

6.631
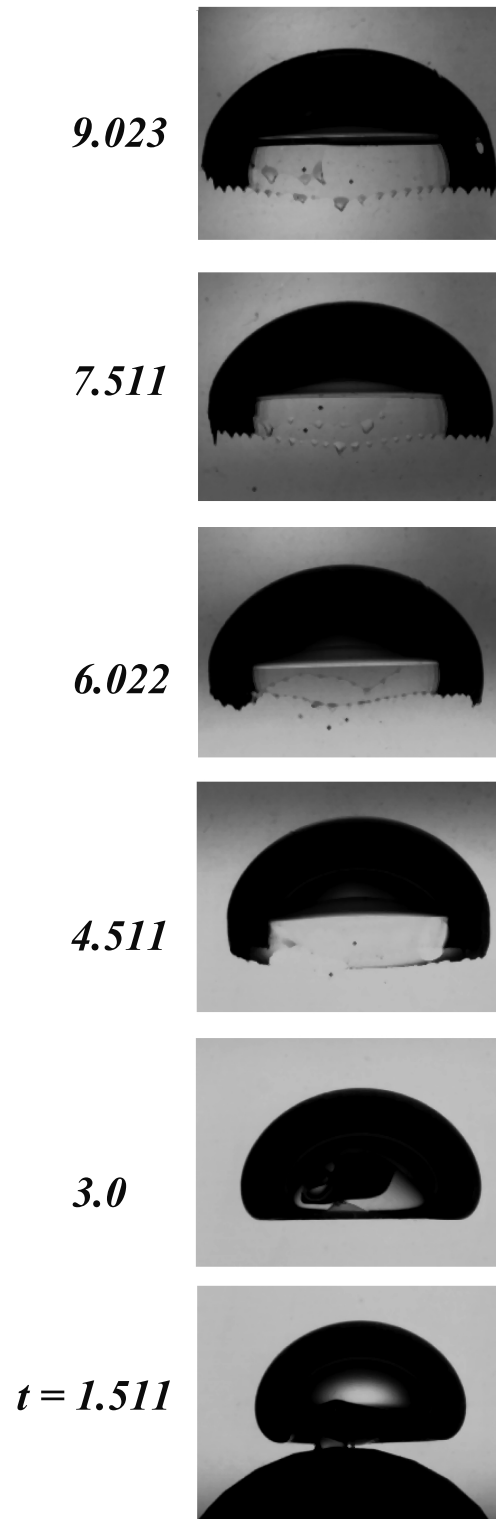
6.028

4.019

2.672

t = 2.009

Figure 4.12: Evolution of shape of regime IV bubble (Peripheral breakup): 80% of glycerol in water, $\mu_r = 1.03 \times 10^{-4}$, $\rho_r = 8.27 \times 10^{-4}$, $R = 24.3$ mm, $Ga = 147.9$ and $Eo = 108.02$

7.030

5.114
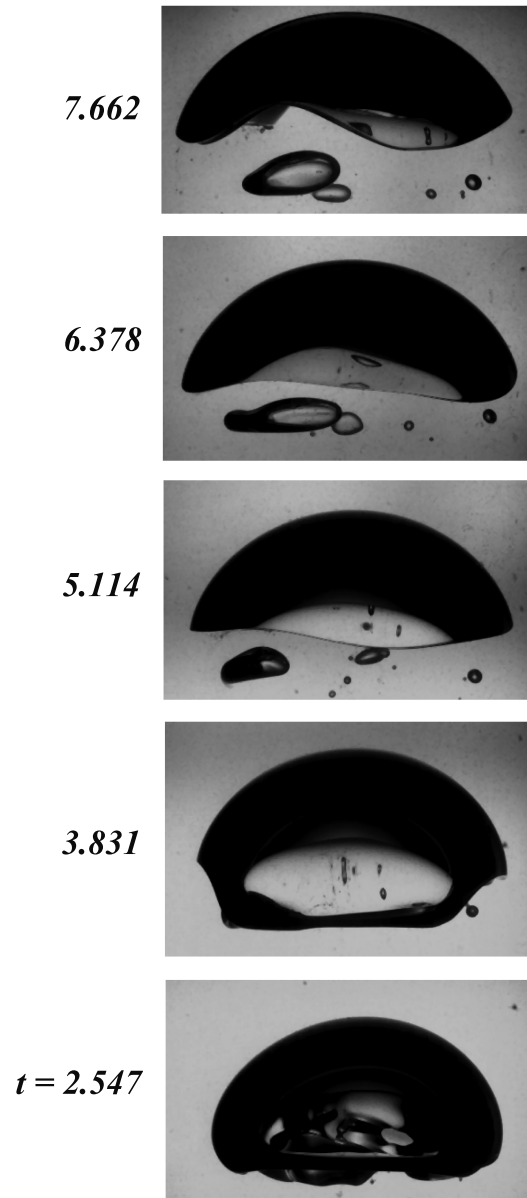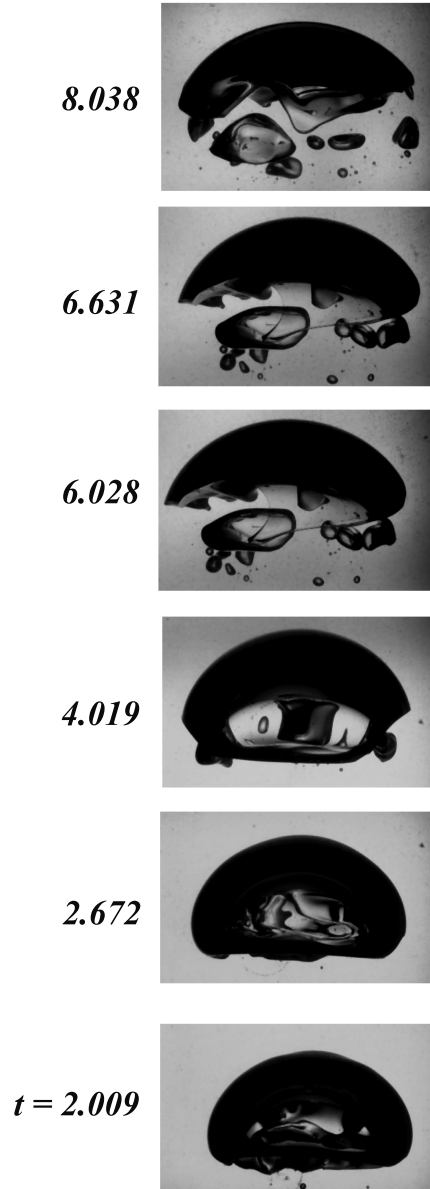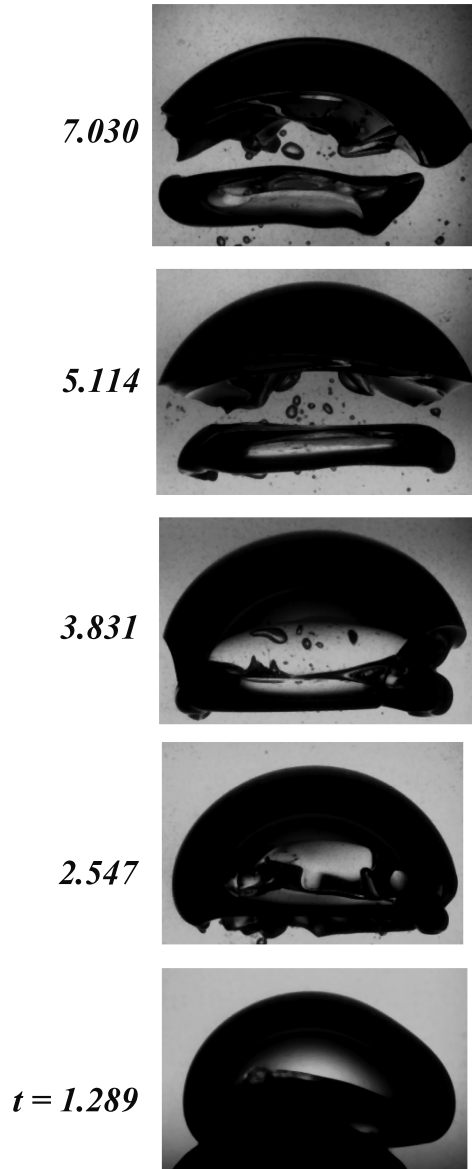
3.831

2.547

t = 1.289

Figure 4.13: Evolution of shape of regime IV bubble (Peripheral breakup): 80% of glycerol in water, $\mu_r = 1.03 \times 10^{-4}$, $\rho_r = 8.27 \times 10^{-4}$, $R = 26.7$ mm, $Ga = 170.82$ and $Eo = 130.85$

Figure 4.6(a) represents a regime IV bubble with skirt breakup. It is clearly visible that before the breakup bubble has a skirt shape similar to regime II. And then as it rises thin skirt part detaches from the main body of bubble to form tiny bubbles in its cap's wake. This skirt is found to collapse in the lateral direction. After the breakup bubble becomes axisymmetric spherical cap shape or a dimple shape as in regime I and it maintain same shape throughout. Figures 4.11, 4.12, and 4.13 represent regime IV bubble with peripheral breakup. Here as the bubble rises its edges breaks off from the main body of bubble to form small satellite bubbles. And after the breakup the bubble possesses an asymmetric shape.

We conducted some parametric study of Eotvos and Galilei numbers with the rise velocity. Here the effect of rise velocity is studied by keeping Eotvos number constant and variable Galilei number, also by keeping Galilei number constant and variable Eotvos number. Some graphs of time vs Z_{tip} were plotted for this purpose.
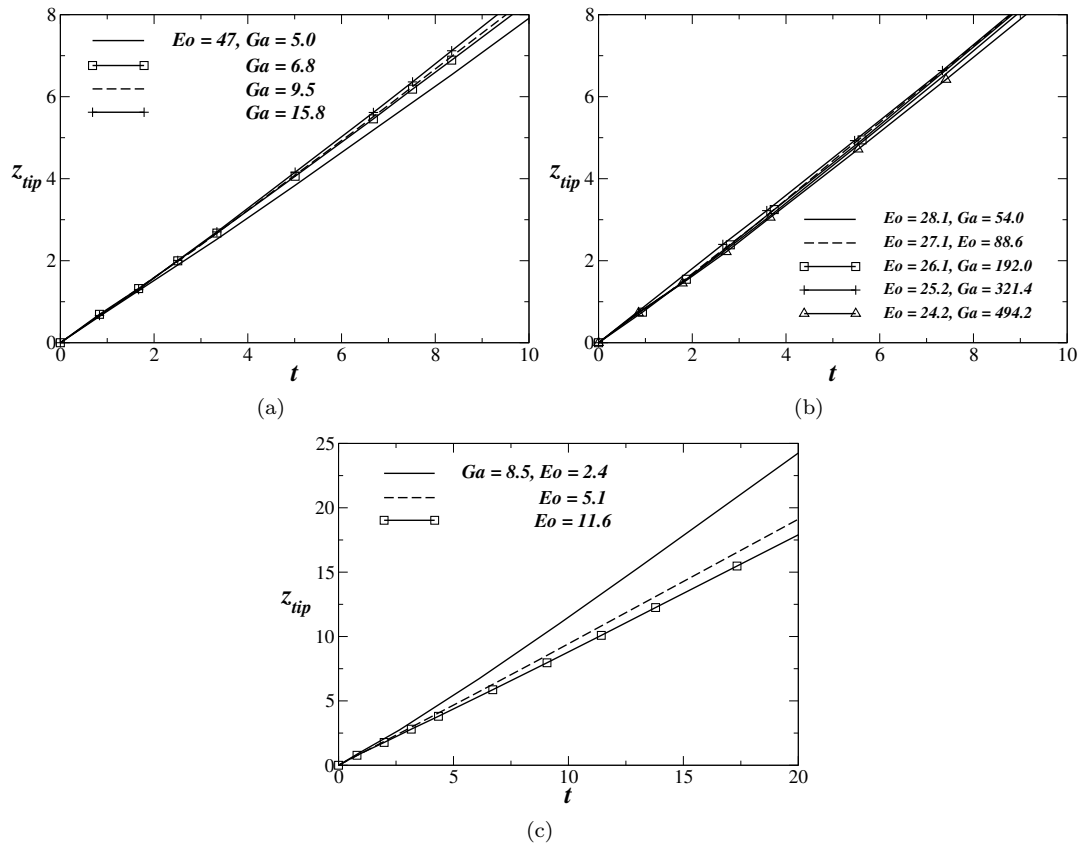
Figure 4.14: Effect of non-dimensional parameters on rise velocity (time,t vs Z_{tip}) : (a) t vs Z_{tip} with Eo=constant (b) t vs Z_{tip} with Eo=constant (c) t vs Z_{tip} with Ga=constant

These plots indicates, by varying Galilei numbers keeping Eotvos number constant (Figure 4.14(a),4.14(b)) the rise velocity of bubbles are almost constant. On the other hand by varying Eotvos number keeping Galilei number constant (Figure 4.14(c)), the bubble with smaller Eotvos number travels at higher rise velocity compared to other ones.

Chapter 5

Conclusion and Future Works

In this thesis we did an experimental study on variation of shape and path of gas bubble rising in fluids of different physical properties. The shape of bubble and the path it follows depends on two non-dimensional numbers, Galilei number and Eotvos number. These numbers are a function of viscosity, density and surface tension of the fluid as well as radius of the bubble. Physical properties of the fluid are changed by choosing aqueous glycerol solution of 18 different concentration and pure millipore water as the fluid medium each having a constant value of Morton number. An experimental setup was fabricated to create initial bubble of different sizes in these liquids and observe its rise behavior using a High-speed camera. A 2D image of the bubble motion is captured through High-speed video recording.

We constructed a phase plot in Galilei - Eotvos plane based on path and shape variation of the rising bubble. This phase plot matches with the one put forward by Tripathi et al. [2] (Figure 2.1) through their numerical simulation of initially spherical air bubble rising in viscous fluid. Unlike Tripathi et al.'s [2] result, our phase plot consist of four different regimes of bubble behavior, while it is five regimes in their phase plot. This discrepancy is because in the numerical simulation Tripathi et al. [2] chose initial shape of the bubble as spherical for all cases, which is practically impossible since larger bubble cannot maintain spherical shape because of its low surface tension compared to high inertia force. Also they kept viscosity and density ratio as constant for all their simulation, while it is varying for each fluid that we chose to conduct the experiments. The bubble is axisymmetric in regime I, asymmetric in regime II and III, and it breaks in regime IV. The two kinds of breakup observed in regime IV are skirted breakup (Figure 4.9) and peripheral breakup (Figure 4.11). Path oscillation is observed only in fluids with Morton number greater than 10^{-3} as explained by [1, 14], and the line corresponding to $Mo = 10^{-3}$ separate regime II and III.

This work can be continued by changing the initial condition of the bubble as hemispherical shape, the shape of dumping cup from which the bubble is released, as well as by taking exact viscosity and density ratio for different fluids, to perform the numerical simulation to get exactly similar phase plot as in Figure 2.1. Also we described regime III bubble as, it is showing path oscillation. But we could not find the nature of oscillation, whether it is zigzag motion or spiral motion. So there is a scope of an experimental study to investigate the nature of oscillation of regime III bubble.

References

[1] D. Bhaga and M. E. Weber. Bubbles in viscous liquids: shapes, wakes and velocities. *J. Fluid Mech* 105, (1981) 6185.

[2] M. K. Tripathi, K. C. Sahu, and R. Govindarajan. Dynamics of an initially spherical bubble rising in quiescent liquid. *Nature Communications* .

[3] L. Bourouiba and J. W. Bush. Drops and Bubbles in the Environment. *Handbook of Environmental Fluid Dynamics* 1, (2013) 427–439.

[4] R. Clift, J. Grace, and M. Weber. Bubbles, Drops and Particles. ACADEMIC PRESS Inc., New York, 1978.

[5] S. Qin, C. F. Caskey, and K. W. Ferrara. Ultrasound contrast microbubbles in imaging and therapy: physical principles and engineering. *Phys Med Biol* .

[6] C. E. Brennen. Cavitation and Bubble dynamics. *Oxford University Press Inc.* .

[7] D. C. Blanchard. The electrification of the atmosphere by particles from bubbles in the sea. *Prog. Oceanogr.* .

[8] A. A. Kulkarni and J. B. Joshi. Bubble Formation and Bubble Rise Velocity in Gas-Liquid Systems: A Review. *Ind. Eng. Chem. Res* 44, (2005) 5873–5931.

[9] A. Prosperetti. Bubbles. *Phys. Fluids* 16.

[10] J. Hua, J. F. Stene, and P. Lin. Numerical Simulation of 3D Bubbles Rising in Viscous Liquids using a Front Tracking Method. *Journal of Computational Physics* 227, (2008) 33583382.

[11] A. Smolianski, H. Haario, and P. Luukka. Numerical study of dynamics of single bubbles and bubble swarms. *Applied Mathematical Modelling* 32, (2008) 641–659.

[12] L. Liu, H. Yan, and G. Zhao. Experimental studies on the shape and motion of air bubbles in viscous liquids. *Experimental Thermal and Fluid Science* 62, (2015) 109–121.

[13] W. L. Haberman and R. K. Morton. An experimental investigation of the drag and shape of air bubbles rising in various liquids. *Technical Report, DTIC Document* .

[14] R. A. Hartunian and W. Searsl. On the instability of small gas bubbles moving uniformly in various liquids. *J. Fluid Mech* 3, (1957) 27–47).

[15] Y. Tagawa, S. Takagi, and Y. Matsumoto. Surfactant effect on path instability of a rising bubble. *J. Fluid Mech* 738, (2014) 124142.

[16] K. Lunde and R. J. Perkins. Shape oscillations of rising bubbles. In Fascination of Fluid Dynamics. *Springer* .

[17] G. Ryskin and L. Leal. Numerical solution of free-boundary problems in fluid mechanics. Part 2. Buoyancy-driven motion of a gas bubble through a quiescent liquid. *J. Fluid Mech* 148, (1984) 19–35.

[18] A. C. Institute. physical properties of glycerine and its solutions. *http://www.aciscience.org/docs/physical-properties-of-glycerine-and-its-solutions.pdf* .